Structural basis of Na+-independent and cooperative substrate/product antiport in CaiT

Schulze, Sabrina; Köster, Stefan; Geldmacher, Ulrike; Terwisscha van Scheltinga, Anke C.; Kühlbrandt, Werner

Published in:
Nature

DOI:
10.1038/nature09310

Publication date:
2010

1. Background

L-carnitine is an essential metabolite in animals, plants, and prokaryotes. *Escherichia coli* and related bacteria, such as *Proteus mirabilis*, use L-carnitine (R(-)-3-hydroxy-4-trimethylaminobutyrate) as an electron acceptor under anaerobic growth conditions and convert it to γ-butyrobetaine[1-4]. Mammalian cells have similar organic cation/carnitine (OCTN) transporters (fig. S1). *E. coli* CaiT is a constitutively active, highly specific L-carnitine/γ-butyrobetaine antiporter, which works in both directions[5]. CaiT belongs to the BCCT (betaine, carnitine, choline transporter) family, which all transport substrates that contain a quaternary ammonium group.

1.1 Trimer architecture

PmCaiT and EcCaiT both form compact trimers of three identical protomers (fig. S3A). A hydrophobic cavity on the cytoplasmic side contains ordered detergent (fig. S3B) and would be filled with – most likely also ordered – lipid in the membrane. As in BetP, the long, curved α-helix 7 (H7) runs along the periplasmic membrane surface. This helix and the loop connecting it to TM8 (loop7, L7b), plus one residue in TM4, mediate tight trimer contacts. Arg299 in H7 forms a salt bridge to Asp288 in the neighbouring protomer. A hydrogen bond connects the hydroxyl of Thr304 in L7b to the backbone carbonyl oxygen of Asn284 the adjacent protomer, and a water molecule connects Asp305 to the backbone amide nitrogen of Gly308 in L7b to Glu132 in TM4. The strong, polar or ionic contacts in the CaiT trimer are thus very different from the hydrophobic trimer contacts in the BetP[6], even though the order and arrangement of helices within the protomers is the same.

1.2 Inverted repeats in CaiT

TM3 to TM7 and TM8 to TM12 in CaiT define the two halves of an inverted repeat (figs. S2A, S4), as in many other secondary transporters[6-12]. The inner core of the protomer is formed by TM3, TM4 of the first repeat and TM8, TM9 of the second repeat, arranged as an antiparallel four-helix bundle (figs. S2A, S4). This inner core is separated by a cytoplasmic

(L4, IH4) and a periplasmic helix-loop-helix motif (EH9a, L9, EH9b) from the supporting framework comprising TM5 to TM7 and TM10 to TM12. TM1 and the curved TM2 form a clamp-like scaffold for the helices of the inverted repeats (fig. S4).

1.3 Role of methionine in substrate coordination

Although the methionine side chain is usually thought of as hydrophobic, it can in fact participate in polar interactions, because the large, uncharged sulfur is more easily polarized than smaller atoms. Two types of interactions are possible[13]. The methionine sulfur is either negatively polarized and behaves as a nucleophile towards positively charged binding partners (e.g. Na^{+}, Ni^{2+}, $H^{\delta+}$, $C^{\delta+}$). Alternatively, the methionine sulfur can be positively polarized and behave as an electrophile towards anions or atoms with a partial negative charge (e.g. Cl^{-}, $O^{\delta-}$). In CaiT the sulfur of Met331 interacts with the negatively charged carboxyl group of γ-butyrobetaine, providing an elegant solution to the problem of recognizing and coordinating a hydrophilic substrate in the hydrophobic protein interior. It is known from the structures of small organic compounds such as 3-(methylthio) propanoic acid or norbornane endo-acid[14] that sulfur atoms in a covalent bond interact with carboxylates[14-16]. Although this interaction does occur in other proteins[17], a functionally important role of such a methionin-carboxylate bridge has not been reported up to now.

2 Tables

Table S1

Structure comparisons of PmCaiT and EcCaiT to each other and to the structurally related transporters BetP, vSGLT and LeuT.

Mol A	Mol B	Z-Score	Aligned Residues	RMSD (Å)	Sequence Identity (%)
PmCaiT (Trimer)	**EcCaiT (Trimer)**	53.6	972	0.9	87
PmCaiT (Protomer)	**EcCaiT (Protomer)**	60.5	496	0.7	87
PmCaiT (Trimer)	**BetP (Trimer)**	43.1	1348	2.2	25
PmCaiT (Monomer)	**BetP (Monomer)**	43.7	478	2.2	25
EcCaiT (Trimer)	**BetP (Trimer)**	37.2	895	2.3	25
EcCaiT (Monomer)	**BetP (Monomer)**	44.0	481	2.2	25
PmCaiT (Monomer)	**vSGLT (Monomer)**	13.7	334	4.2	13
EcCaiT (Monomer)	**vSGLT (Monomer)**	13.6	333	4.0	12
PmCaiT (Monomer)	**LeuT (Monomer)**	14.8	342	4.1	10
EcCaiT (Monomer)	**LeuT (Monomer)**	14.7	335	4.3	10

Table S2

Lookup table for trans-membrane helices in LeuT-type transporters. TM3 to TM7 in CaiT or BetP are the equivalent of helices 1 to 5, and TM8 to TM12 are the equivalent of helices 6 to 10 in the other transporters.

	CaiT	BetP	vSGLT	LeuT	Mhp1	AdiC	ApcT
Repeat 1							
Helix 1	87 – 118	137 – 169	52 – 80	10 – 38	28 – 55	11 – 37	9 – 37
Helix 2	127 – 163	177 – 212	83 – 109	40 – 72	57 – 86	43 – 67	40 – 66
Helix 3	186 – 224	234 – 268	123 – 158	87 – 125	99 – 137	81 – 112	83 – 117
Helix 4	228 – 249	275 – 296	161 – 178	165 – 185	142 – 159	122 – 143	122 – 141
Helix 5	251 – 277	300 – 325	185 – 213	189 – 214	161 – 191	146 – 172	145 – 172
Repeat 2							
Helix 6	311 – 340	358 – 390	249 – 277	240 – 269	208 – 234	195 – 217	183 – 214
Helix 7	343 – 377	393 – 427	279 – 314	275 – 306	241 – 278	226 – 248	218 – 247
Helix 8	403 – 435	448 – 482	348 – 385	336 – 371	295 – 331	277 – 310	269 – 305
Helix 9	445 – 467	488 – 511	391 – 418	374 – 396	335 – 351	323 – 342	320 – 337
Helix 10	469 – 502	513 – 546	422 – 448	398 – 425	359 – 383	351 – 376	339 – 364

Table S3

Kinetic and substrate binding analysis of wildtype (wt) PmCaiT, PmCaiT mutants, and wt EcCaiT.

	PmCaiT				EcCaiT
	wt	E111A	W316A	M331V	wt
Transport					
K_M (μM)	46 ± 6 119.7 ± 20 [a)]	inactive	159.2 ± 10.8	123.3 ± 12.2	81.1 ± 11.8 100.4 ± 14.1 [a)]
v_{max} (nmol substrate/ (min•mg protein))	4672 ± 205 4824 ± 301 [a)]		1816 ± 353	478 ± 53	4921 ± 243 4975 ± 243 [a)]
k_{cat} (L-carnitine/min)	263 ± 12 272 ± 17 [a)]		69 ± 4	26 ± 3	279 ± 14 282 ± 14 [a)]
Substrate binding (detergent solution)					
K_D (γ-butyrobetaine) (mM)	3.1 ± 0.6 3.4 ± 0.2 [a)]		17.5 ± 6.0	11.7 ± 1.2 11.8 ± 1.7 [a)]	3.9 ± 0.7
B_{max} (γ-butyrobetaine) (mM)	42.6 ± 2.4 42.0 ± 1.0 [a)]		58.6 ± 7.8	51.1 ± 3.0 50.2 ± 2.8 [a)]	43.3 ± 3.2
Hill coefficient	1.0 ± 0.1		0.9 ± 0.1	1.1 ± 0.1	1.0 ±0.1
K_D (L-carnitine) (mM)	1.8 ± 0.3 2.4 ± 0.4 [a)]		9.0 ± 1.3	7.1 ± 1.1 7.0 ± 0.8 [a)]	1.9 ± 0.2
B_{max} (L-carnitine) (mM)	40.3 ± 2.5 39.1 ± 2.3 [a)]		33.7 ± 1.3	41.7 ± 2.7 45.1 ± 1.5 [a)]	39.1 ± 3.1
Hill coefficient	1.1 ± 0.1		1.0 ± 0.1	1.1 ± 0.1	1.2 ± 0.1
Substrate binding (proteoliposomes)					
K_D (γ-butyrobetaine) (mM)	5.6 ± 0.8		11.2 ± 1.7	n.d. [b)]	5.3 ± 0.8
B_{max} (γ-butyrobetaine) (mM)	34.3 ± 2.9		21.8 ± 1.8	n.d.	22.8 ± 0.8
Hill coefficient	1.5 ± 0.1		1.7 ± 0.2	n.d.	1.4 ± 0.1
K_D (L-carnitine) (mM)	4.5 ± 0.8		7.5 ± 1.2	n.d.	5.8 ± 1.0
B_{max} (L-carnitine) (mM)	28.2 ± 1.9		24.4 ± 0.8	n.d.	30.5 ± 1.5
Hill coefficient	1.4 ± 0.1		1.6 ± 0.1	n.d.	1.5 ± 0.2

[a)] Measurements in presence of 50 mM NaCl;. [b)] not determined

Table S4

Data collection and phasing statistics

	P. mirabilis CaiT	*E. coli* CaiT
Beamline	X10SA SLS	X10SA SLS
Wavelength (Å)	0.92	0.98
Resolution (Å) [a)]	19.7 – 2.3 (2.4 – 2.3)	24.7 – 3.4 (3.6 -3.4)
Cell dimensions	$a = b = 129.2$ Å, $c = 160.3$ Å $\alpha = \beta = 90^\circ$, $\gamma = 120^\circ$	$a = b = 124.20$ Å, $c = 154.63$ Å $\alpha = \beta = 90^\circ$, $\gamma = 120^\circ$
Number of measured reflections	246 131	136 423
Number of unique reflections	43 243	71 232
Completeness (%)	97.7 (91.2)	97.7 (87.1)
Redundancy	5.7	1.9
$I/\sigma(I)$	9.0 (1.4)	12.8 (1.3)
R_{merge} (%) [b)]	8.4 (55.7)	6.0 (90.0)
R_{work} (%) [c)]	20.9	23.7
R_{free} (%) [d)]	23.8	27.1
r.m.s. deviations		
Bond length (Å)	0.007	0.011
Bond angles (°)	0.980	1.302

[a)] Numbers in parentheses represent statistics for data in the highest resolution shell

[b)] $R_{merge} = \Sigma_{hkl}\Sigma_i ||F_{hkl}| - |F_{hkl}(i)|| / \Sigma_{hkl}\Sigma_i|F_{hkl}(i)|$

[c)] $R_{work} = \Sigma_{hkl}||F_{obs}| - k|F_{calc}|| / \Sigma_{hkl}|F_{obs}|$

[d)] R_{free} was calculated with 5% of reflections not used during refinement.

3 Supplementary figures

Figure S 1

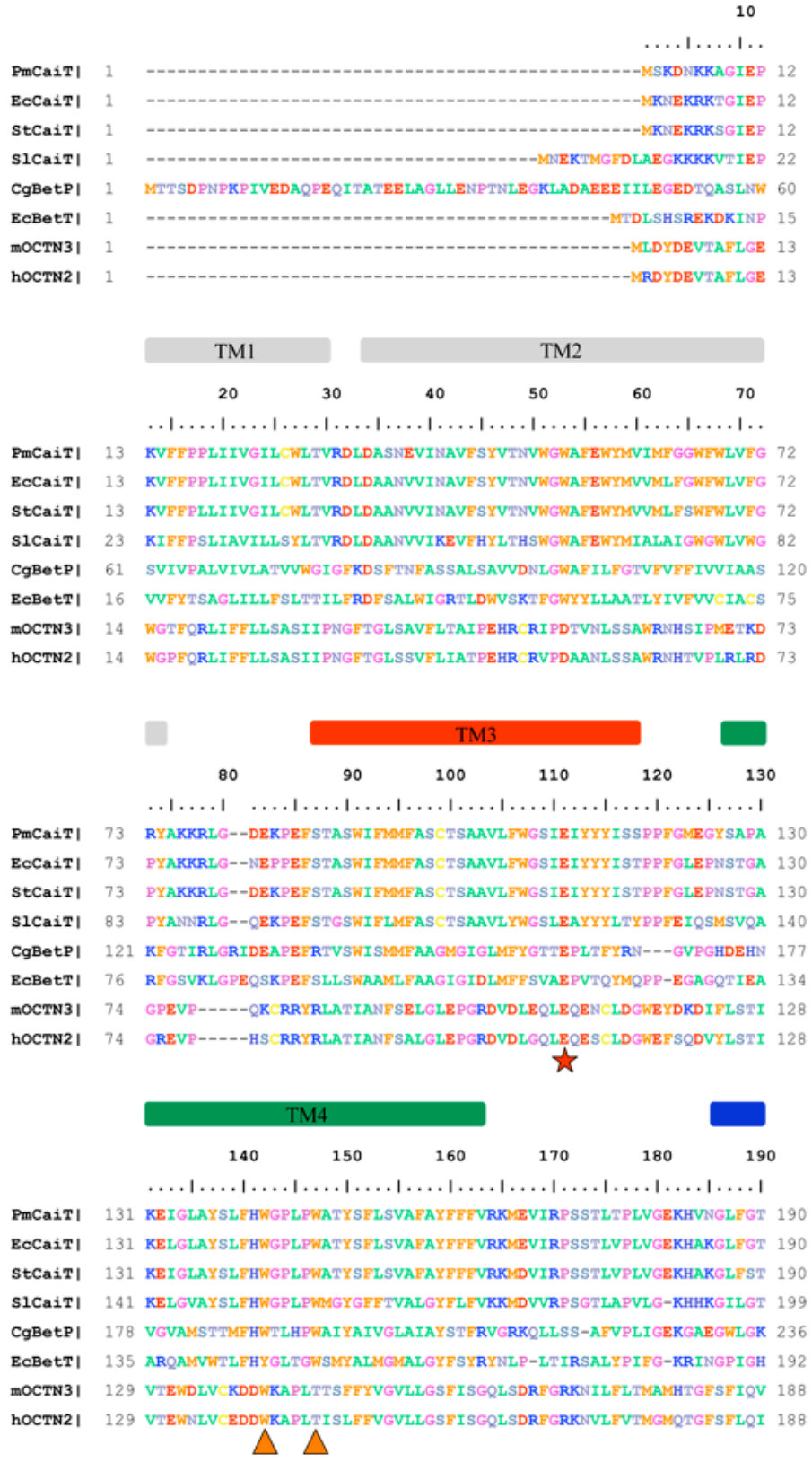

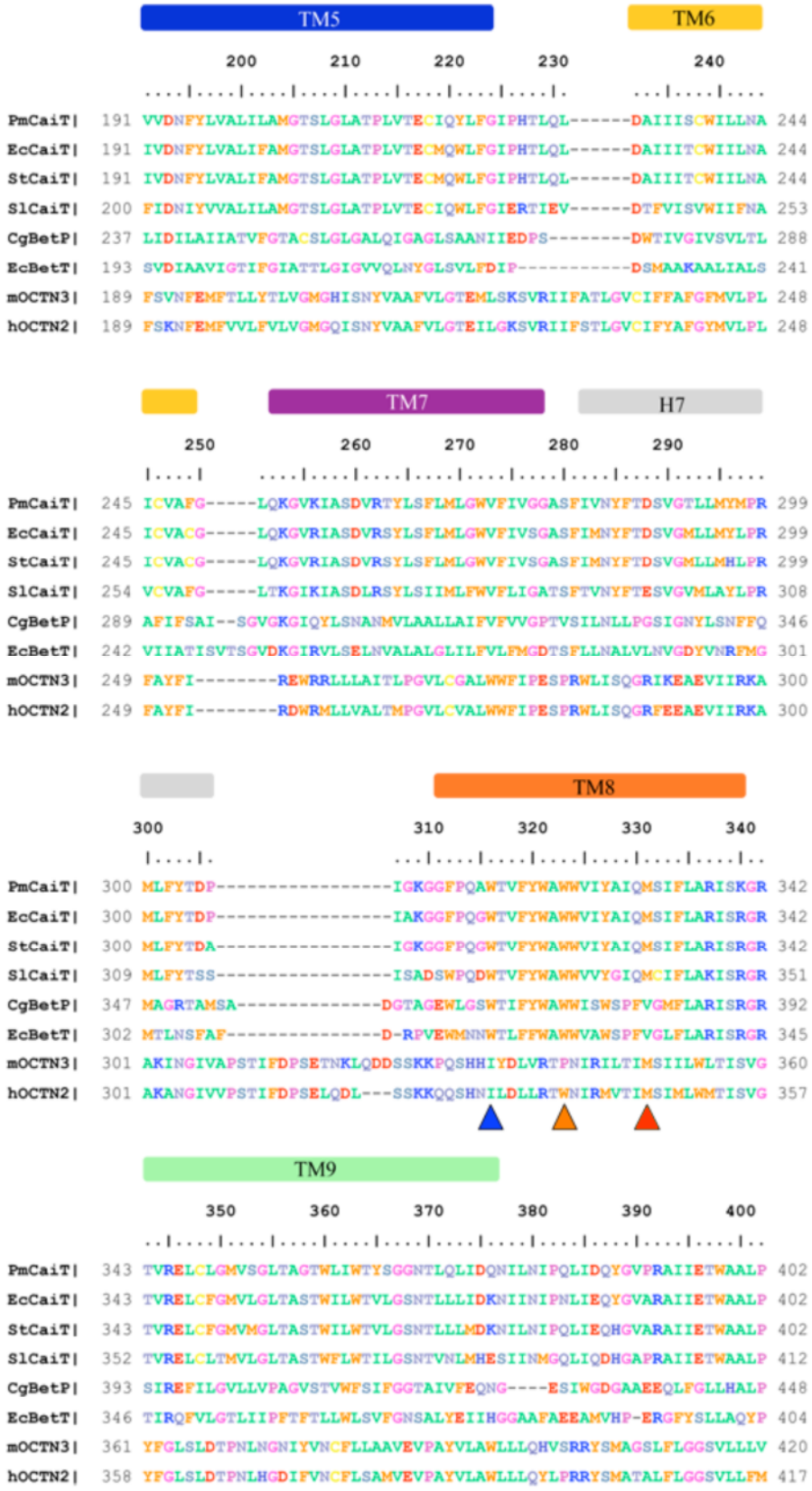
TM5
TM6
200 210 220 230 240
PmCaiT| 191 VVDNFYLVALILAMGTSLGLATPLVTECIQYLFGIPHTLQL------DAIIISCWILLNA 244
EcCaiT| 191 IVDNFYLVALIFAMGTSLGLATPLVTECMQWLFGIPHTLQL------DAIIITCWIILNA 244
StCaiT| 191 IVDNFYLVALIFAMGTSLGLATPLVTECMQWLFGIPHTLQL------DAIIITCWIILNA 244
SlCaiT| 200 FIDNIYVVALILAMGTSLGLATPLVTECIQWLFGIERTIEV------DTFVISVWIIFNA 253
CgBetP| 237 LIDILAIIATVFGTACSLGLGALQIGAGLSAANIIEDPS--------DWTIVGIVSVLTL 288
EcBetT| 193 SVDIAAVIGTIFGIATTLGIGVVQLNYGLSVLFDIP----------DSMAAKAALIALS 241
mOCTN3| 189 FSVNFEMFTLLYTLVGMGHISNYVAAFVLGTEMLSKSVRIIFATLGVCIFFAFGFMVLPL 248
hOCTN2| 189 FSKNFEMFVVLFVLVGMGQISNYVAAFVLGTEILGKSVRIIFSTLGVCIFYAFGYMVLPL 248
TM7
H7
250 260 270 280 290
PmCaiT| 245 ICVAFG-----LQKGVKIASDVRTYLSFLMLGWVFIVGGASFIVNYFTDSVGTLLMYMPR 299
EcCaiT| 245 ICVACG-----LQKGVRIASDVRSYLSFLMLGWVFIVSGASFIMNYFTDSVGMLLMYLPR 299
StCaiT| 245 ICVACG-----LQKGVRIASDVRSYLSFLMLGWVFIVSGASFIMNYFTDSVGMLLMHLPR 299
SlCaiT| 254 VCVAFG-----LTKGIKIASDLRSYLSIIMLFWVFLIGATSFTVNYFTESVGVMLAYLPR 308
CgBetP| 289 AFIFSAI--SGVGKGIQYLSNANMVLAALLAIFVFVVGPTVSILNLLPGSIGNYLSNFFQ 346
EcBetT| 242 VIIATISVTSGVDKGIRVLSELNVALALGLILFVLFMGDTSFLLNALVLNVGDYVNRFMG 301
mOCTN3| 249 FAYFI--------REWRRLLLAITLPGVLCGALWWFIPESPRWLISQGRIKEAEVIIRKA 300
hOCTN2| 249 FAYFI--------RDWRMLLVALTMPGVLCVALWWFIPESPRWLISQGRFEEAEVIIRKA 300
TM8
300 310 320 330 340
PmCaiT| 300 MLFYTDP----------IGKGGFPQAWTVFYWAWWVIYAIQMSIFLARISKGR 342
EcCaiT| 300 MLFYTDP----------IAKGGFPQGWTVFYWAWWVIYAIQMSIFLARISRGR 342
StCaiT| 300 MLFYTDA----------IGKGGFPQGWTVFYWAWWVIYAIQMSIFLARISRGR 342
SlCaiT| 309 MLFYTSS----------ISADSWPQDWTVFYWAWWVVYGIQMCIFLAKISRGR 351
CgBetP| 347 MAGRTAMSA----------DGTAGEWLGSWTIFYWAWWISWSPFVGMFLARISRGR 392
EcBetT| 302 MTLNSFAF----------D-RPVEWMNNWTLFFWAWWVAWSPFVGLFLARISRGR 345
mOCTN3| 301 AKINGIVAPSTIFDPSETNKLQDDSSKKPQSHHIYDLVRTPNIRILTIMSIILWLTISVG 360
hOCTN2| 301 AKANGIVVPSTIFDPSELQDL---SSKKQQSHNILDLLRTWNIRMVTIMSIMLWMTISVG 357
TM9
350 360 370 380 390 400
PmCaiT| 343 TVRELCLGMVSGLTAGTWLIWTYSGGNTLQLIDQNILNIPQLIDQYGVPRAIIETWAALP 402
EcCaiT| 343 TVRELCFGMVLGLTASTWILWTVLGSNTLLLIDKNIINIPNLIEQYGVARAIIETWAALP 402
StCaiT| 343 TVRELCFGMVMGLTASTWILWTVLGSNTLLLMDKNILNIPQLIEQHGVARAIIETWAALP 402
SlCaiT| 352 TVRELCLTMVLGLTASTWFLWTILGSNTVNLMHESIINMGQLIQDHGAPRAIIETWAALP 412
CgBetP| 393 SIREFILGVLLVPAGVSTVWFSIFGGTAIVFEQNG----ESIWGDGAAEEQLFGLLHALP 448
EcBetT| 346 TIRQFVLGTLIIPFTFTLLWLSVFGNSALYEIIHGGAAFAEEAMVHP-ERGFYSLLAQYP 404
mOCTN3| 361 YFGLSLDTPNLNGNIYVNCFLLAAVEVPAYVLAWLLLQHVSRRYSMAGSLFLGGSVLLLV 420
hOCTN2| 358 YFGLSLDTPNLHGDIFVNCFLSAMVEVPAYVLAWLLLQYLPRRYSMATALFLGGSVLLFM 417

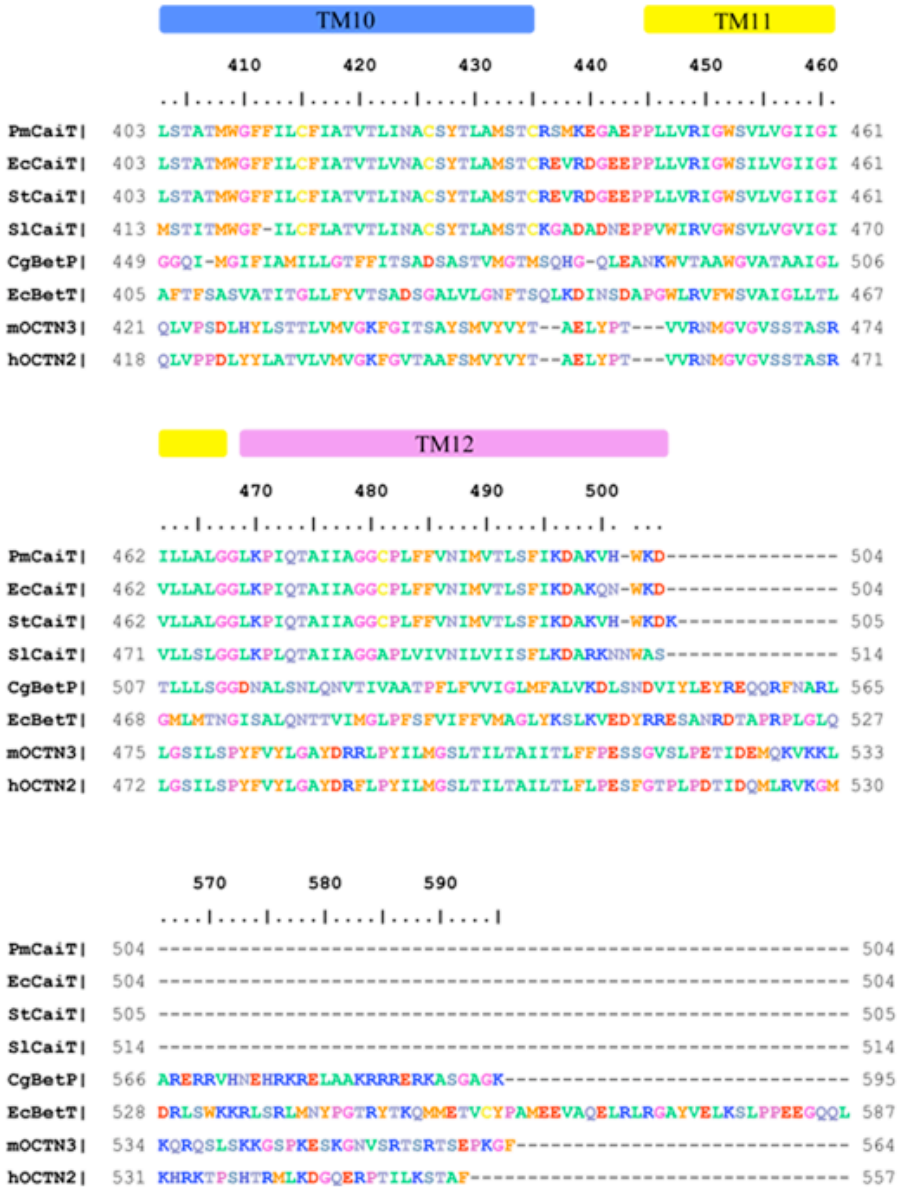

Amino acid sequence alignment of CaiT from *Proteus mirabilis* (PmCaiT), *E. coli* (EcCaiT), *Salmonella typhimorium* (StCaiT), *Shewanella loihica* (SlCaiT), BetP from *Corynebacterium glutamicum* (CgBetP), *E.coli* BetT (EcBetT), and organic cation transporters from mouse (mOCTN3) and human (hOCTN2). Red triangle: Met331 which coordinates the carboxyl group of the bound substrate in the transport site of CaiT. Orange triangles: fully or partly conserved hydrophobic residues in the central transport site. Blue triangle: Trp316 in the regulatory site of CaiT. Red asterisk: Glu111, which coordinates the network of hydrogen bonds linking the two inverted repeats in the inside-open conformation of CaiT (Fig. 4a,b). Residues 588 – 677 of EcBetT were omitted.

Figure S 2

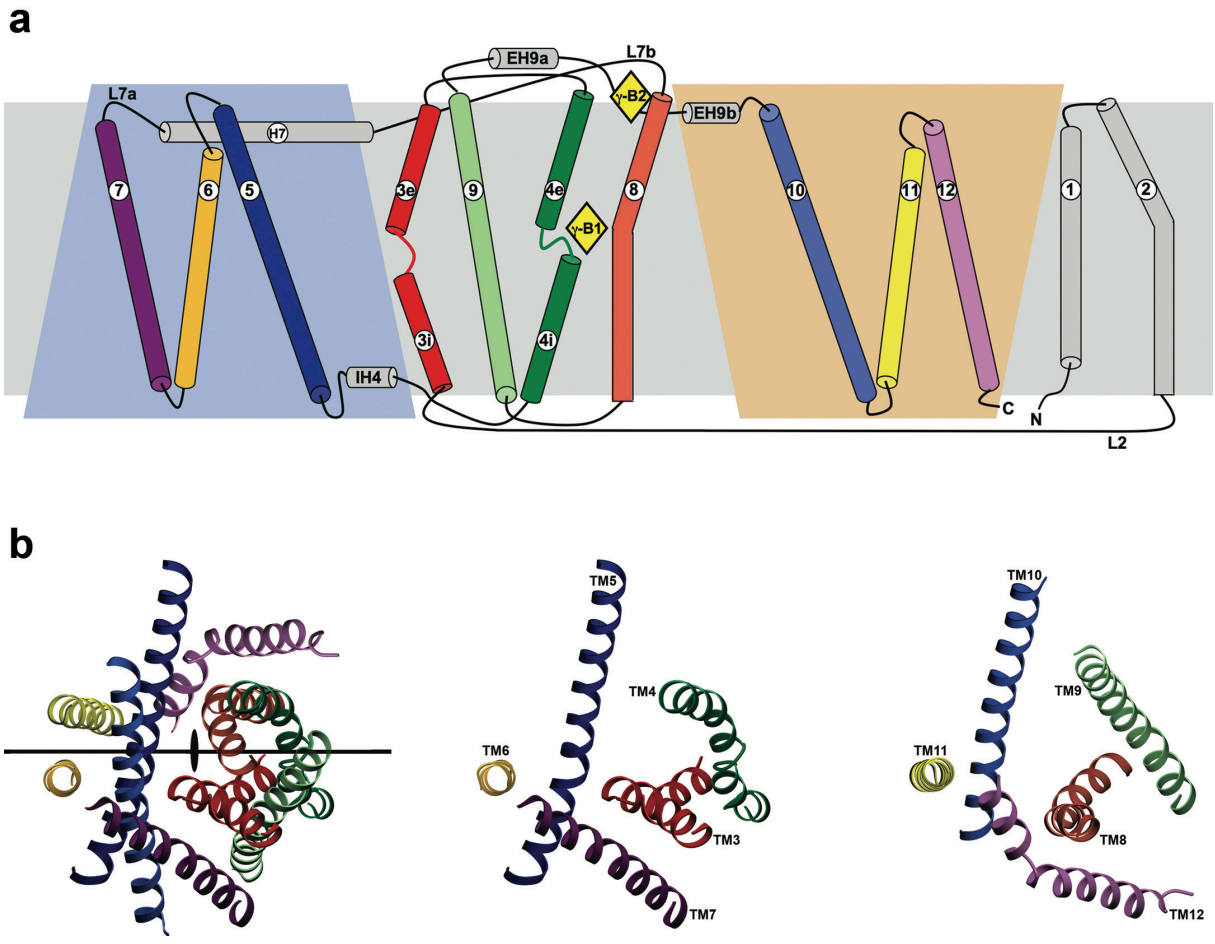

(a) Inverted helix repeats in CaiT. Repeat 1 (TM3 to TM7) is shown in dark colours, repeat 2 (TM8 to TM12) in lighter colours.

(b) The 10 TM helices of the two inverted repeats (left) are coloured as in (a). Repeat 2 (right) is rotated relative to repeat 1 (centre) by ~180° around the internal pseudo-twofold axis of the protomer (black line), and by ~20° in the perpendicular direction.

Figure S 3

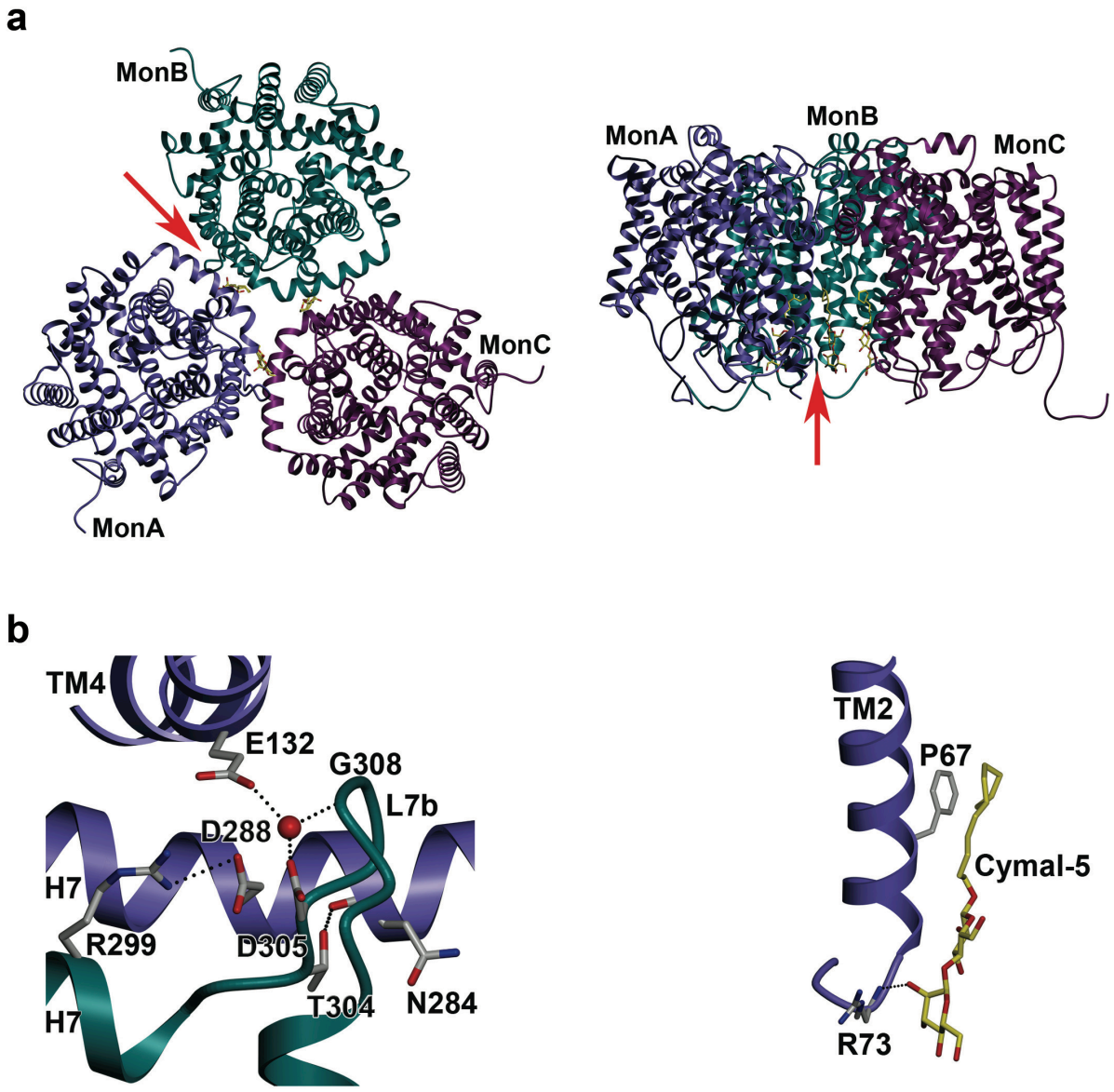

(a) The PmCaiT trimer. In the periplasmic view (left), close contacts between protomers (arrow) are mediated by an ion pair (yellow sidechains) and hydrogen bonds. The side view (right) shows a deep cavity between protomers on the cytoplasmic side (arrow) that contains bound detergent (yellow). (b) Detailed views of the ion and water bridges that connect protomers in the trimer (left), and the Cymal-5 detergent head group interacting with the aromatic sidechain of Phe67 (right) in the hydrophobic cavity.

Figure S 4

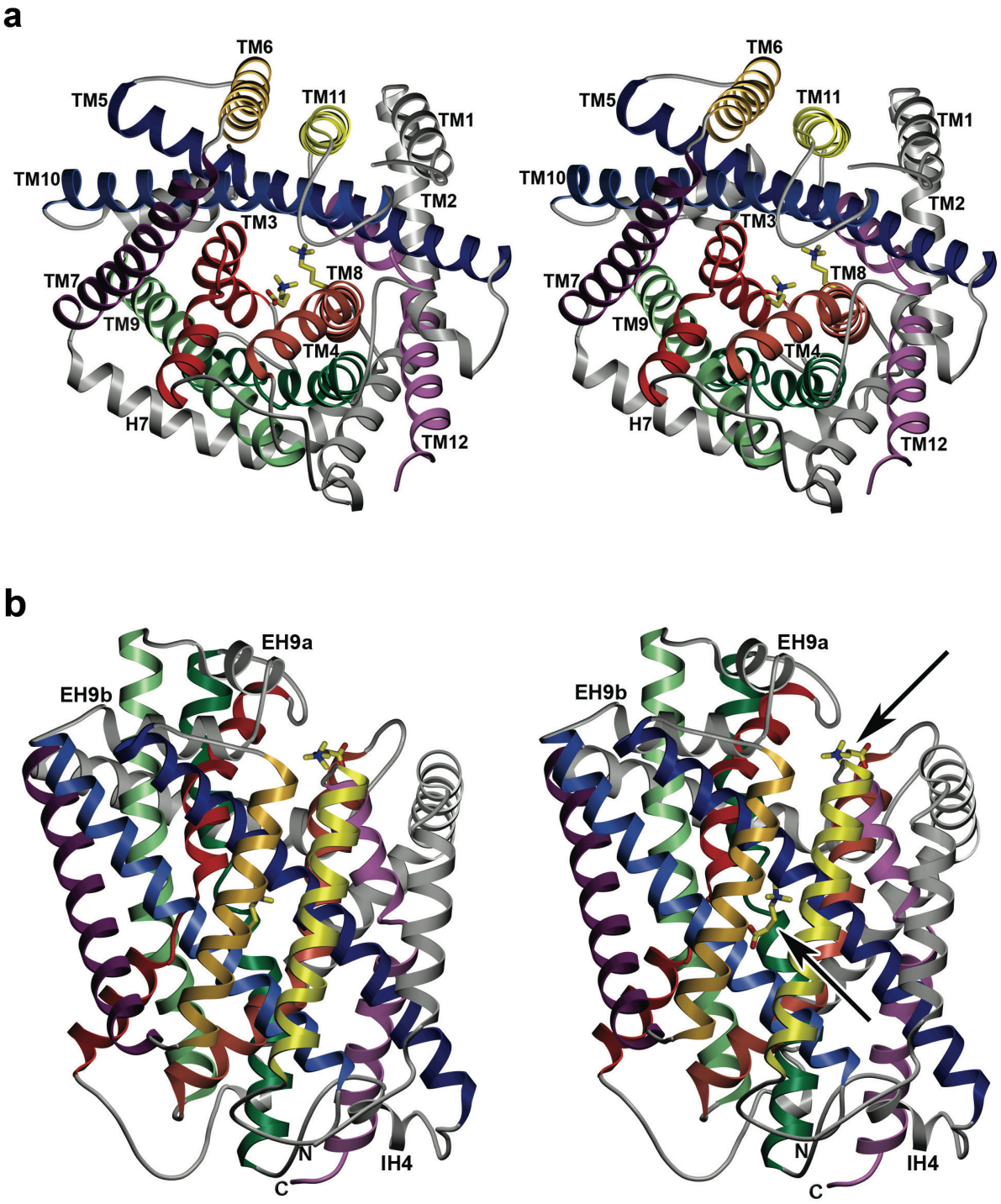

Stereo diagrams of the EcCaiT protomer with two bound γ-butyrobetaine substrates. (a) cytoplasmic view; (b) side view. The arrows in B point to the bound substrate molecules in the transport site (centre) and in the regulatory site on the periplasmic side.

Figure S 5

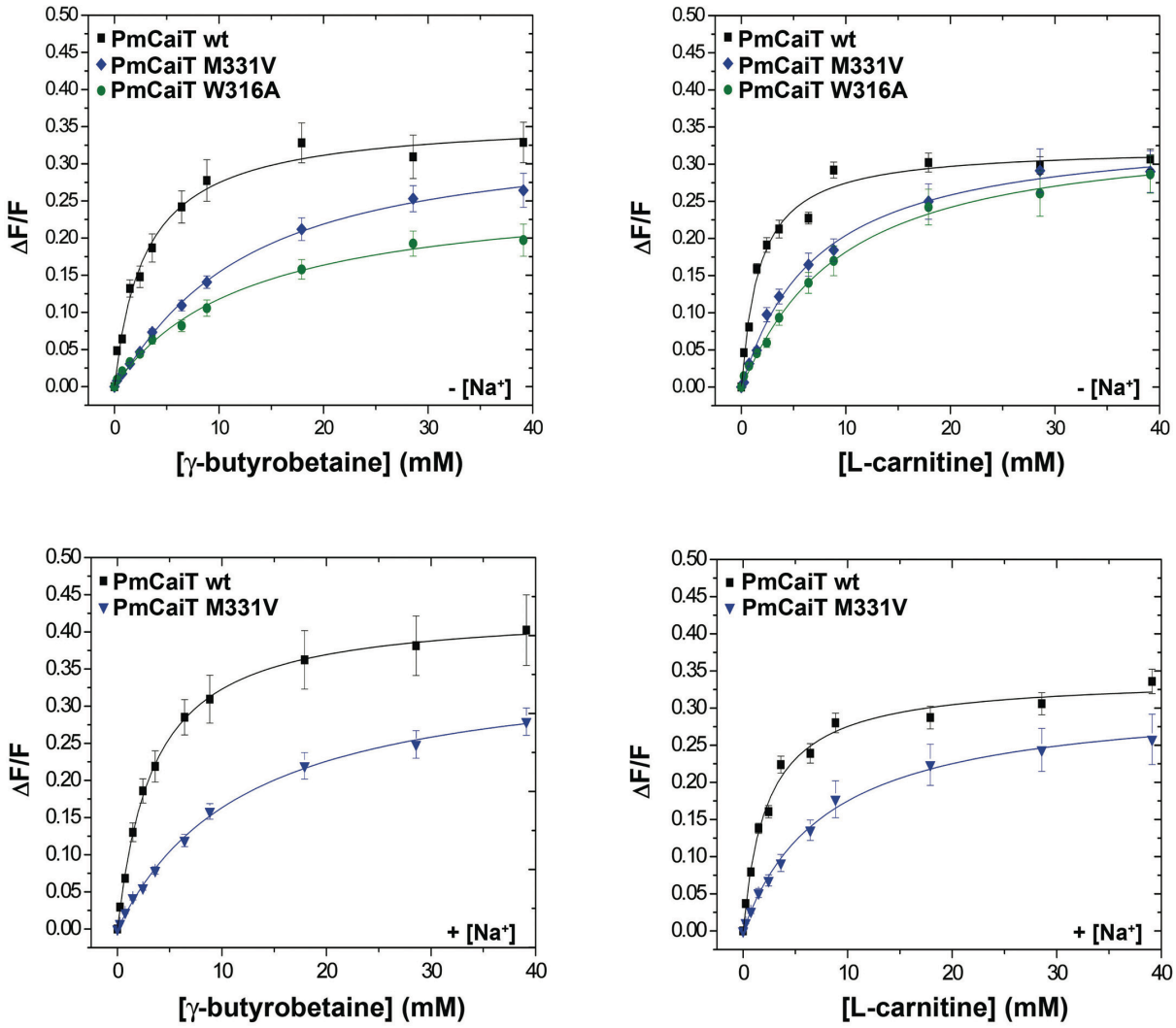

Binding of γ-butyrobetaine or L-carnitine to wildtype (wt) PmCaiT (black), PmCaiT M331V (blue) and PmCaiT W316A (green) solubilised in the detergent Cymal-5 in sodium-free buffer (top) or with 50 mM NaCl, monitored by Trp fluorescence.

Figure S 6

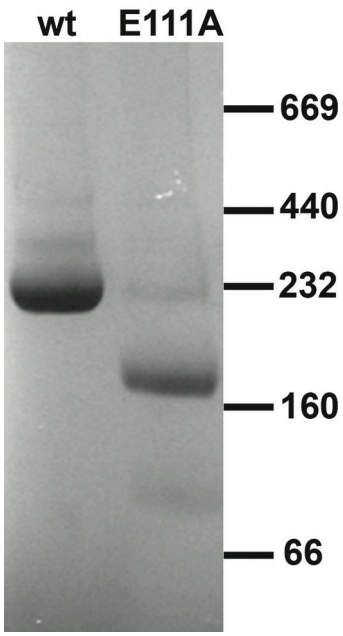

Oligomeric state of CaiT in detergent solution. Wildtype PmCaiT (wt) forms stable trimers that run at about 230 kDa in the blue-native gradient gel (4 – 16%). Mutation of Glu111 to alanine (E111A) destabilizes the trimer, and results in the appearance of dimers and monomers.

Figure S 7

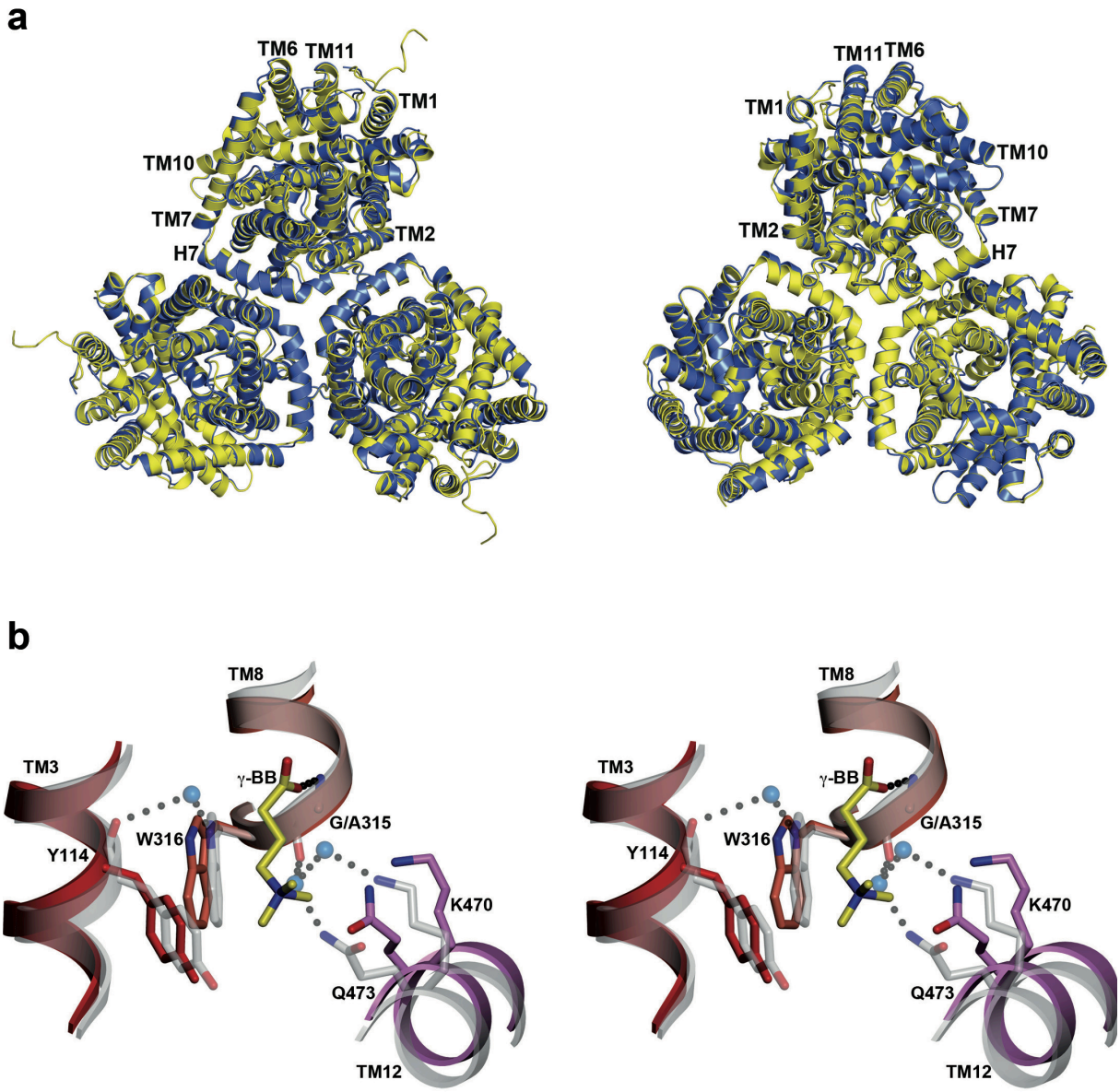

(a) Cytoplasmic (left) and extracellular view (right) of the PmCaiT trimer (yellow) superposed onto the EcCaiT trimer (blue) in stereo. The superposition indicates a 3° tilt of the substrate-bound EcCaiT protomer relative to PmCaiT, towards the threefold axis in the extracellular view. (b) Stereo view of the superimposed regulatory sites of EcCaiT (coloured) and PmCaiT (grey). Substrate binding in the external binding site replaces two water molecules and disrupts the hydrogen bond network coordinated by them. As a result, the extracellular end of TM12 moves by ~1.3Å.

Figure S 8

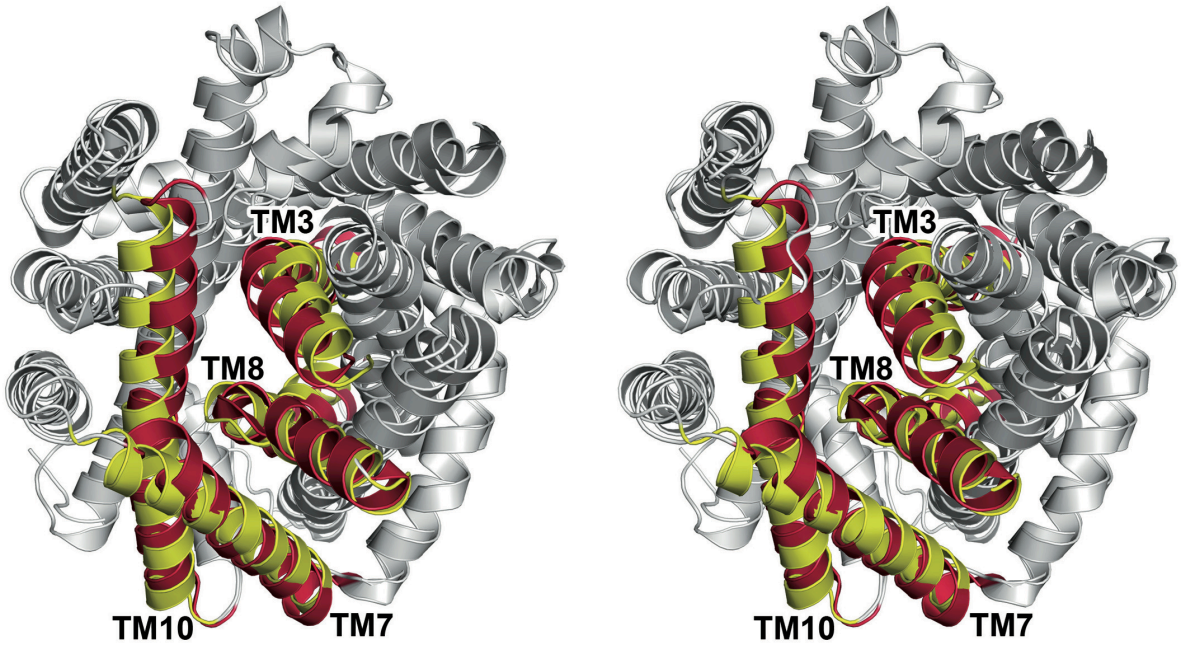

Stereo drawing of superposed protomers of PmCaiT and BetP, showing an iris-like movement of the cytoplasmatic part of the helices TM3, TM7, TM8 and TM10 (yellow for PmCaiT, red for BetP) in the transition from the fully inside-open conformation of CaiT to the occluded state of BetP.

Figure S 9

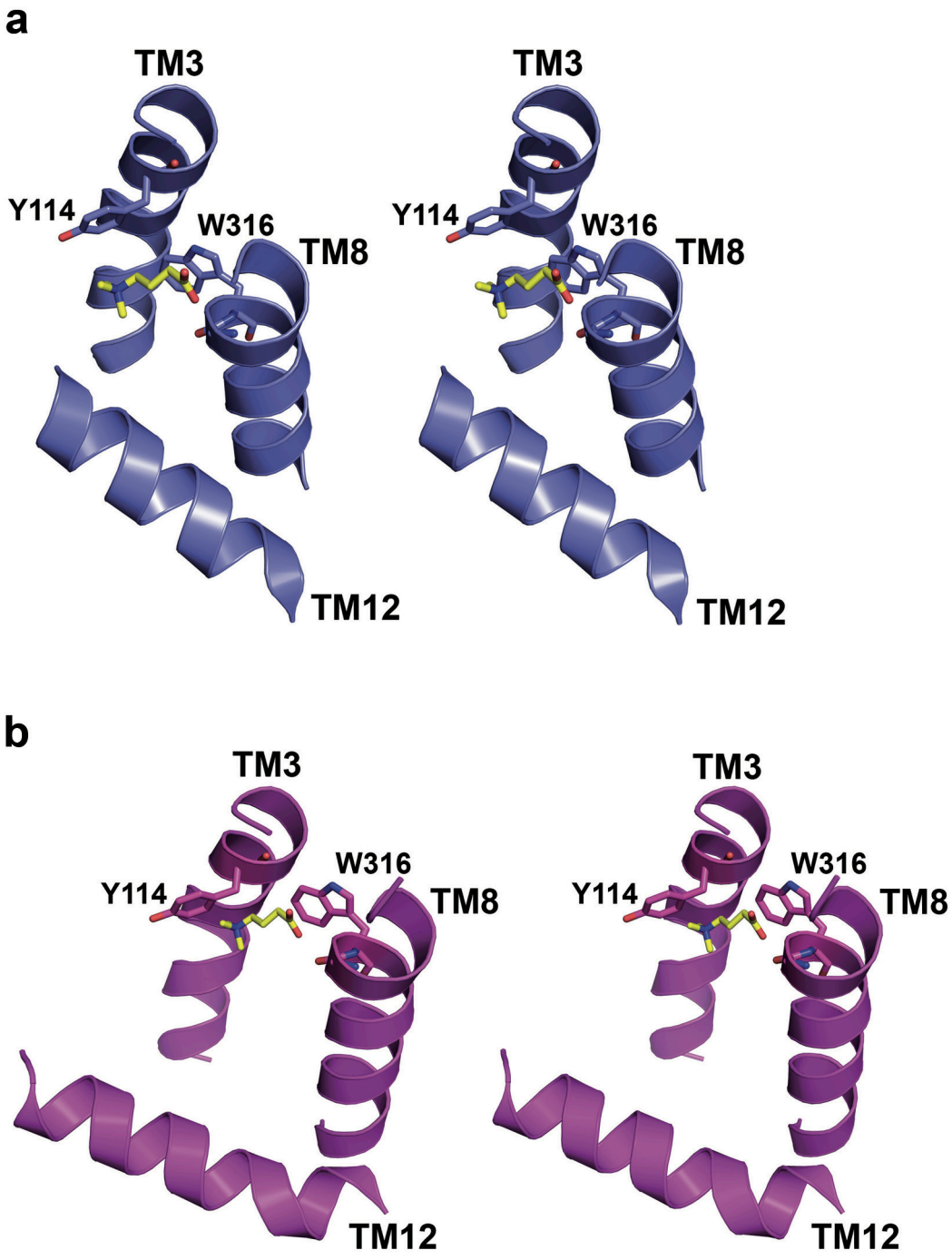
a
TM3
Y114
W316
TM8
TM12
TM3
Y114
W316
TM8
TM12
b
TM3
W316
Y114
TM8
TM12
TM3
W316
Y114
TM8
TM12

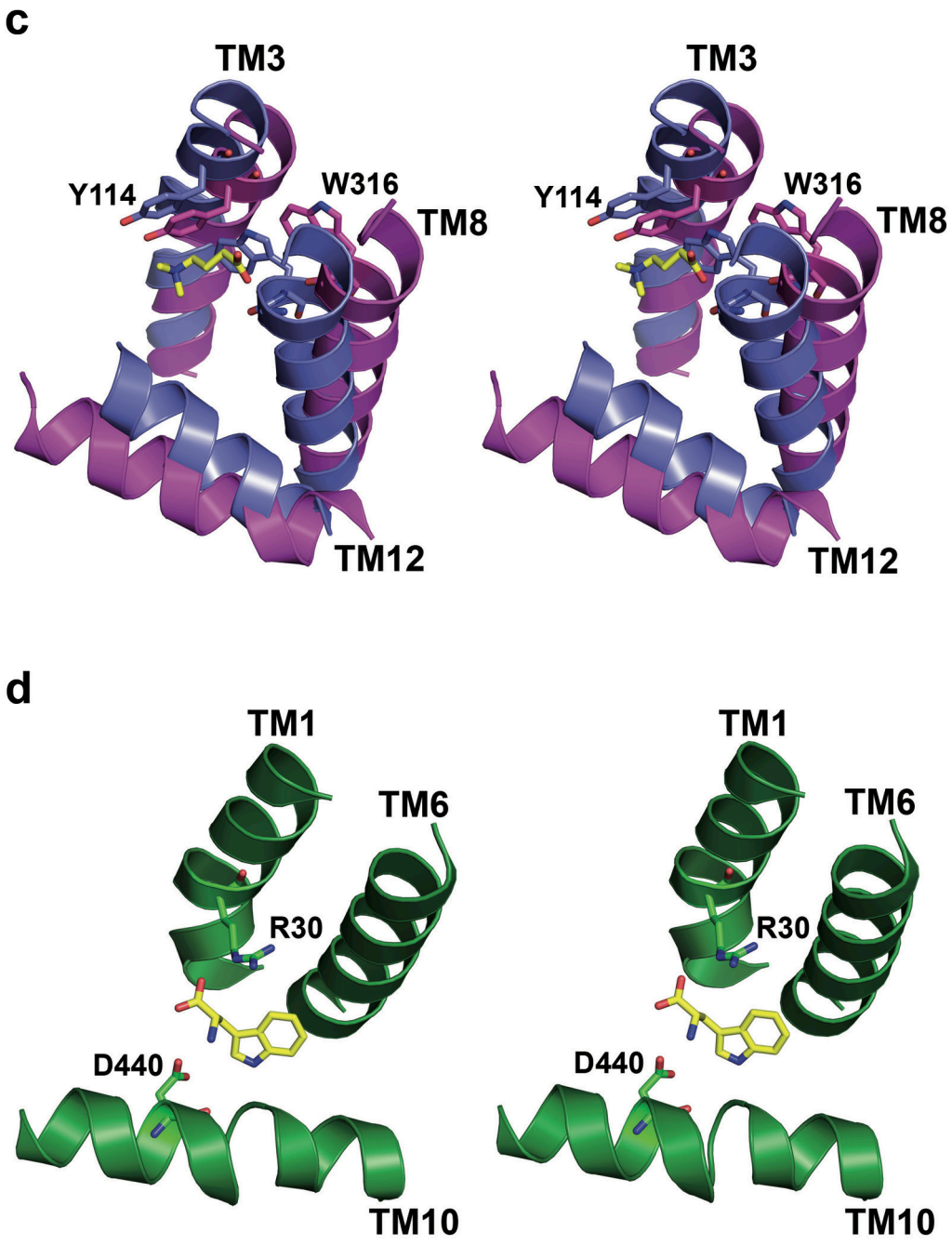

Stereo drawings comparing EcCaiT helices TM3, TM8 and TM12 with key residues in the inside-open conformation (a, blue) to a model of EcCaiT in the outside-open conformation (b, pink), based on the LeuT structure. In the model (b), the second, regulatory substrate-binding site on the extracellular side defined by residues Tyr114, Trp316 and the carbonyl oxygen of Gly315 remains intact, so that substrate is likely to remain bound throughout the transport cycle. (c) Superposition of A and B, indicating the helix movements that accompany the transition from the inside-open to the outside-open conformation on the extracellular side of CaiT. (d) Corresponding helix regions of the outside-open LeuT (TM1, TM6 and TM10,

green) in complex with tryptophan. The Trp in the extracellular channel of LeuT is in a different position compared to the substrate in the regulatory site of CaiT.

4. References

1. Jung, H., Jung, K. & Kleber, H. P. L-carnitine metabolization and osmotic stress response in Escherichia coli. *J Basic Microbiol* **30**, 409-413 (1990).
2. Jung, H., Jung, K. & Kleber, H. P. L-carnitine uptake by Escherichia coli. *J. Basic. Microbiol.* **30**, 507-514 (1990).
3. Jung, K., Jung, H. & Kleber, H. P. Regulation of L-carnitine metabolism in Escherichia coli. *J. Basic. Microbiol.* **27**, 131-137 (1987).
4. Kleber, H. P. Bacterial carnitine metabolism. *FEMS Microbiol. Lett.* **147**, 1-9, doi:S0378-1097(96)00412-0 [pii] (1997).
5. Jung, H. *et al.* CaiT of Escherichia coli, a new transporter catalyzing L-carnitine/gamma -butyrobetaine exchange. *J Biol Chem* **277**, 39251-39258, doi:10.1074/jbc.M206319200M206319200 [pii] (2002).
6. Ressl, S., Terwisscha van Scheltinga, A. C., Vonrhein, C., Ott, V. & Ziegler, C. Molecular basis of transport and regulation in the Na(+)/betaine symporter BetP. *Nature* **458**, 47-52, doi:nature07819 [pii]10.1038/nature07819 (2009).
7. Faham, S. *et al.* The crystal structure of a sodium galactose transporter reveals mechanistic insights into Na+/sugar symport. *Science* **321**, 810-814, doi:1160406 [pii]10.1126/science.1160406 (2008).
8. Gao, X. *et al.* Structure and mechanism of an amino acid antiporter. *Science* **324**, 1565-1568, doi:1173654 [pii]10.1126/science.1173654 (2009).
9. Sevilla, A. *et al.* Design of metabolic engineering strategies for maximizing L-(-)-carnitine production by Escherichia coli. Integration of the metabolic and bioreactor levels. *Biotechnol. Prog.* **21**, 329-337, doi:10.1021/bp0497583 (2005).
10. Weyand, S. *et al.* Structure and molecular mechanism of a nucleobase-cation-symport-1 family transporter. *Science* **322**, 709-713, doi:1164440 [pii]10.1126/science.1164440 (2008).
11. Yamashita, A., Singh, S. K., Kawate, T., Jin, Y. & Gouaux, E. Crystal structure of a bacterial homologue of Na+/Cl--dependent neurotransmitter transporters. *Nature* **437**, 215-223, doi:nature03978 [pii]10.1038/nature03978 (2005).
12. Fang, Y. *et al.* Structure of a prokaryotic virtual proton pump at 3.2 A resolution. *Nature* **460**, 1040-1043, doi:nature08201 [pii]10.1038/nature08201 (2009).
13. Rosenfield, J., R.E., Parthasarathy, R. & Dunitz, J. D. Directional Preferences of Nonbonded Atomic Contacts with Divalent Sulfur. 1. Electrophiles and Nucleophiles. *J. Am. Chem. Soc.* **99**, 4860-4862 (1977).
14. Mahling, S., Asmus, K. D., Glass, R. S., Hojjatie, M. & Wilson, G. S. Neighboring group participation in radicals: pulse radiolysis studies on radicals with sulfur-oxygen interaction. *J. Org. Chem.* **52**, 3717-3724 (1987).
15. Burling, F. T. & Goldstein, B. M. A database study of nonbonded intramolecular sulfur-nucleophile contacts. *Acta Crystallogr. B* **49 (Pt 4)**, 738-744 (1993).
16. Pal, D. & Chakrabarti, P. Non-hydrogen bond interactions involving the methionine sulfur atom. *J. Biomol. Struct. Dyn.* **19**, 115-128 (2001).
17. Pal, D. & Chakrabarti, P. Non-hydrogen bond interactions involving the methionine sulfur atom. *J Biomol Struct Dyn* **19**, 115-128 (2001).